



## **THERMOSOLUTAL CONVECTION IN A RECTANGULAR ENCLOSURE WITH VERTICAL MIDDLE-PARTITIONS**

**L.W. Wang<sup>1</sup> Y.S. Chen<sup>2</sup> J.K. Sung<sup>2</sup> Y.C. Kung<sup>3</sup>**

### **ABSTRACT**

The current study is primarily motivated to gain better understanding of the flow pattern, the temperature and concentration distributions caused by thermosolutal convection in an electrochemical system with a vertical middle partitions. The test cell is a rectangular enclosure formed with acrylic and copper plates, which is wrapped with foam insulator to ensure an adiabatic boundary condition, and its aspect ratio is 2. The temperature is kept constant and controlled by two separated constant-temperature baths, which circulate heated or cooled water through the heat exchanger. The working solution inside this test cell is aqueous copper sulphate. An electrochemical method based on a diffusion controlled electrode reaction will be employed in this work for creating the concentration gradient. To visualize the flow pattern, the shadowgraph technique is used. Finally, the correlations between Sherwood number and  $Gr_m$ ,  $Gr_t$  are also need to be analyzed. The results show that the flow velocity is increased due to the blocks. In the thermalsolutal convection (opposing case), it's observed the finger type flow happened near two copper plates.

**Keywords: Thermosolutal Convection, Shadowgraphy, Rectangular Enclosure**

### **INTRODUCTION**

This work investigates flows that are caused by buoyancy forces due to combined temperature and species concentration effects in an annular enclosure with steps. Natural convection heat transfer in an enclosure occurs in numerous practical situations, such as electronic equipment cooling by natural convection, heat loss from a solar collector, convection in building elements, convection during crystal growth and fluid-filled thermal storage tanks. Convection in which the buoyant forces are caused by both temperature and concentration gradients is normally called thermosolutal convection or double-diffusive convection. As indicated by Ostrach (1980), various modes of convection are possible, depending on how temperature and concentration gradients are oriented relative to each other as well as to gravity. Wang et al. (1983) conducted an experiment on this problem in which a copper sulfate-acid

---

<sup>1</sup> Corresponding author: College of General Studies, Yuan Ze University, Taoyuan, Taiwan, R.O.C,  
Email: [melwlv@saturn.yzu.edu.tw](mailto:melwlv@saturn.yzu.edu.tw), Tel.:+886-3-4353290, Fax: +886-3-435-1006

<sup>2</sup> Department of Mechanical Engineering, Yuan-Ze University, Taoyuan, Taiwan, R.O.C, Email: [s965008@mail.yzu.edu.tw](mailto:s965008@mail.yzu.edu.tw)

<sup>3</sup> System Development III, Taiwan Systems and Technology Laboratory, IBM, Tel.:+886-2-81706312  
Email: [yckung@tw.ibm.com](mailto:yckung@tw.ibm.com)

solution (CuSO<sub>4</sub>+H<sub>2</sub>SO<sub>4</sub>+H<sub>2</sub>O) was used. Kamotani et al. (1985) used an electrochemical system to establish a horizontal concentration gradient in the enclosure. A three-layered flow structure was observed in the enclosure due to the combined driving force. Convection in stratified fluids with imposed horizontal temperature gradients in rectangular enclosures has also been studied, such as by Ostrach (1982).

Although the above studies have addressed thermosolutal phenomena for a rectangular cavity, the rectangular cavity within partitions also has important engineering geometry, particularly for energy storage devices and metal castings. However, the lack of information on the thermosolutal natural convective heat transfer in the rectangular cavity within partitions motivates the present investigation.

This investigation attempts to examine convection by the combined effects of temperature and concentration gradients in a rectangular enclosure with vertical middle-partitions. A CuSO<sub>4</sub> + H<sub>2</sub>SO<sub>4</sub> + H<sub>2</sub>O solution is used as the working fluid. The large difference between the thermal and solutal diffusion rates causes the flow to exhibit double-diffusive characteristics. The parameters herein study are Pr =7 , Sc =1700~2500 , Ar =2 , Ap =1/2 , Gr<sub>t</sub> =3.27×10<sup>6</sup> , Gr<sub>m</sub> =3.49×10<sup>7</sup> , |N|=10.68

## EXPERIMENTAL DESIGN

### Dimensionless Parameters

Given the basic differential equation for thermosolutal convection in a rectangular enclosure with vertical middle-partitions, the following dimensionless parameters are important in this problem:

$$Ap=(W-2s)/W \quad \text{Aperture Ratio}$$

$$Ar=H/W \quad \text{Aspect Ratio}$$

$$Gr_t \equiv g\beta\Delta CH^3/\nu^2 \quad \text{thermal Grashof number}$$

$$Pr \equiv \nu/\alpha \quad \text{Prandlt number}$$

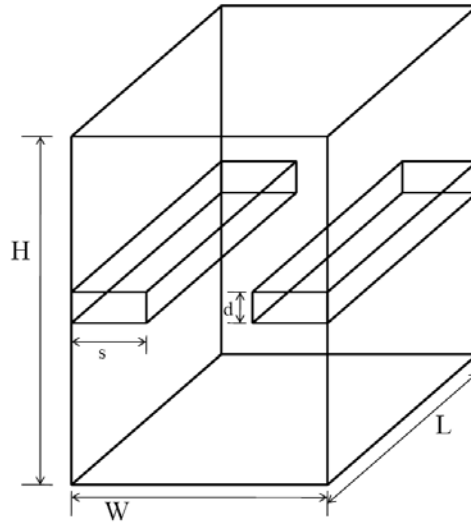
$$Sc \equiv \nu/D \quad \text{Schmidt number}$$

$$N \equiv \bar{\beta}\Delta C/\beta\Delta T \quad \text{buoyancy ratio}$$

where  $g$  is the gravitational acceleration;  $\nu$  denotes the fluid kinematic viscosity;  $\alpha$  is the thermal diffusivity, and  $D$  is the diffusion coefficient. The height of the enclosure are  $H$ , respectively.  $\Delta T$  and  $\Delta C$  are the imposed temperature and concentration differences, respectively. The density variation due to temperature is represented as a volumetric thermal expansion coefficient  $\beta$ . The density variation due to the concentration is presented using the volumetric solutal expansion coefficient  $\bar{\beta}$ . The ( $Gr_t$ ,  $Gr_m$ ) combination is sometimes used instead of the ( $Gr_t$ ,  $N$ ) combination, where  $Gr_m$  is defined as

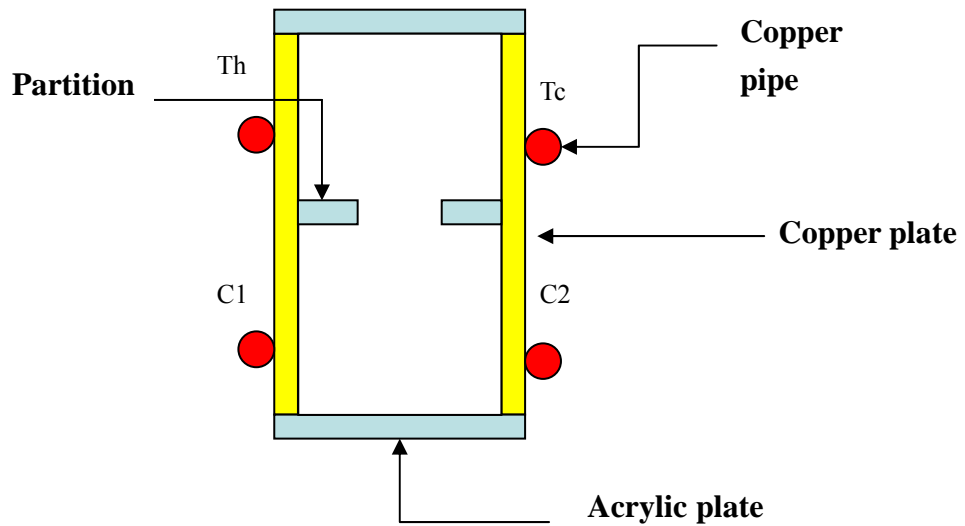
$$Gr_m \equiv g \bar{\beta} \Delta C H^3 / \nu^2 = N Gr_t \quad (1)$$

**Test Apparatus and Procedure**



H	W	L	d	s	Ar	Ap
72mm	36mm	130mm	3mm	9mm	2	1/2

**(a) The test cell**



**(b)**

**Fig. 1. Illustration of experimental system**

Fig. 1 schematically presents the experimental system. The test cell was a rectangular enclosure, consisting of two vertical partitions placed at the middle of left and right plate, and two Plexiglas windows. The depth of the enclosure was L=130 mm. The right and left plate were cooled or heated by

circulating water from two constant-temperature baths that were used to maintain the temperature of the working fluid to within  $\pm 0.1^\circ\text{C}$ . Six thermocouples were embedded into the case to measure the temperature uniformity over the entire surface. The complete setup was enclosed in fiberglass insulation to minimize heat loss from the system into the surrounding environment. The left and right plate temperatures were carefully adjusted from the mean operating temperature  $(T_h+T_c)/2$  to the ambient temperature, within  $\pm 10^\circ\text{C}$  of the ambient air, to minimize the thermal interaction of the apparatus with its surroundings. Some of the insulation could be removed to facilitate qualitative observations of the flow structure. The copper polarities were switched to realize the cooperating and opposing cases. In the first case, the directions of the thermal and solutal diffusion direction were identical, allowing the thermal and solutal buoyancy to cooperate (cooperating case). In the second case, the thermal and solutal diffusion directions opposed each other (opposing case).

### Electrochemical System

In this study, an electrochemical method that is based on a diffusion-controlled electrode reaction is used to create the concentration gradient. A copper sulfate solution is the electrolyte. A DC power supply is used to provide the desired current to initialize electrolysis between the electrodes. A digital multimeter and a recorder are connected in parallel to the electronic circuit to measure the temporal variation of potential and the current. When a voltage is applied to the electrodes, the copper dissolves into the solution at the anode and is deposited at the cathode.

Cupric ion dissolved at the anode:



Cupric ion deposited at the cathode



Consequently, the density of the fluid near the cathode (anode) became smaller (bigger) than that of the bulk solution and an upward flow of solution was produced. The circumstances at the anode were the reverse. In the electrochemical deposition, the transport of the reactant, which could be charged, proceeded by three mechanisms - convection, diffusion and electrical migration. Experimentally, the electrical migration complicates the problem at hand. Hence, adding sulfuric acid to the solution, which acts as a supporting electrolyte, eliminates the migration of the cupric ion in the electrical field. Supporting the electrolyte in the solution increases the conductivity of the solution and thereby reduces the electric field and, therefore, the transference number in the solution. The transference number is defined as the fraction of the current that is carried by an ion (in the absence of concentration variations), and in this case is estimated to be approximately 0.001. Therefore, the migration term is negligible. The mass transfer of minor species is then primarily due to diffusion and convection, as described by Tobias et al. (1953) and Newman (1991). One relatively simple way to specify the

concentration level at the cathode wall in this system is to adjust the cell potential such that the current saturates (reaches the limiting value) is obtained (Fig. 2). The rate of the cupric ion transfer per unit area is

$$n = h_c (C_b - C_0) \quad (4)$$

Since the current that flows between the two electrodes is proportional to the reaction rate, the transport problem is reduced to the measurement of an electrical current:

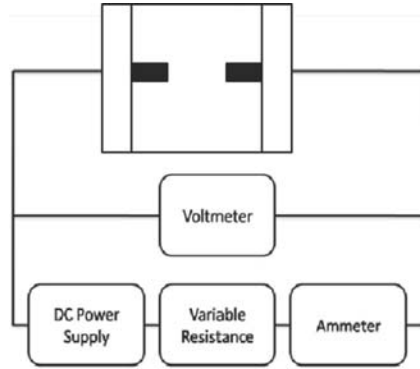


**Fig. 2. Circuit diagram for electrochemical system**

$$n = \frac{i}{bF} \quad (5)$$

where  $i$  is the current density;  $F$  is Faraday's constant, and  $b$  is the charge number of the reacting ions. Equations (4) and (5) yield,

$$h_c = \frac{i}{bF(C_b - C_0)} \quad (6)$$

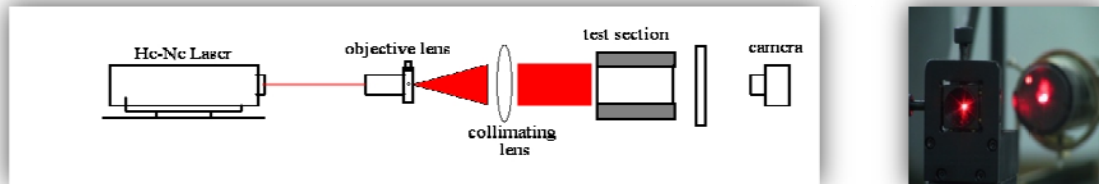
Since  $C_b$  is the concentration in the bulk fluid and  $C_0$  is generally unknown, the limiting current conditions ( $C_0=0$ ) must be applied; that is, the system must be operated at the maximum current density that is allowed for the exclusive production of the desired electrode reaction. Then,

$$h_c = \frac{i_L}{bFC_b} \quad (7)$$

This is the equation that is used to calculate the mass transfer rate in an electrochemical system. At the limiting current condition, the change in concentration across the solutal boundary layer along the cathode is  $\Delta C_{\text{cathode}} = C_b$

## Laser Optical System

The shadowgraph technique is adopted primarily to visualize the growth of the interface between layers. A light beam from a 35mW He-Ne laser is expanded with a spatial filter and then collimated through a large-diameter plane convex lens (Fig. 3).



(a) Diagram for optical system (b) Photograph of laser and lens

**Fig. 3. Laser optical system**

The collimated light that passes through a region with a large refractive index variation is deflected and causes a shadow on the screen. The salt finger structure and the interface between layers in a flow with a relatively large variation in refractive index can be clearly observed. A Nikon D100 professional digital camera is used for photographing. This technique is based on the idea that the intensity of a light beam that is absorbed by the solution is proportional to the solution concentration as the light beam passes through the solution.

## RESULTS AND DISCUSSION

### Boundary Setup

In this section, an experiment is performed with a working solution of copper-sulfate acid solution, ( $\text{CuSO}_4 + \text{H}_2\text{SO}_4 + \text{H}_2\text{O}$ ) to investigate the flow motion of thermosolutal convection in a rectangular enclosure with vertical middle-partitions. However, the flow regime classification holds for both working solutions used herein study - aqueous  $\text{CuSO}_4$  and  $\text{CuSO}_4 + \text{H}_2\text{SO}_4$  - except in that the buoyancy ratio for the formation of the layered structure differs between the solutions. For fixed  $Ar=2$ ,  $Ap=1/2$  and  $Gr_m = 3.49 \times 10^7$ , different  $Gr_t$  numbers, copper polarities, observations and flow pattern photographs are obtained at the limiting current. This section discusses in detail the flow patterns and mass transfer rate. The mass transfer is initiated after 8 hours in a thermally steady state and the photographs and the data recorded every 10min, 30min, 60min, 120min and 180 min in each case. Notably,  $t=0$  is the time at which the limiting current condition initially applies. In this study, the hot and cold walls are held at the left and right plate of the rectangular enclosure, respectively. The following two cases are established; (1) the left plate is the cathode and the right plate is the anode; (2) the left plate is the anode and the right plate is the cathode. The former is the cooperating case and the latter is the opposing case. Fig. 4. presents the boundary conditions.

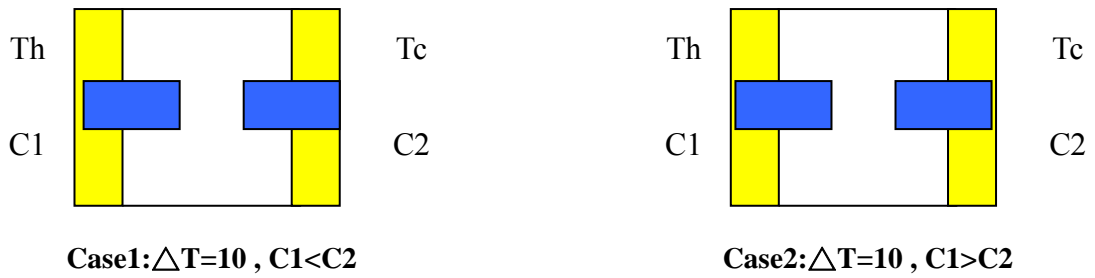
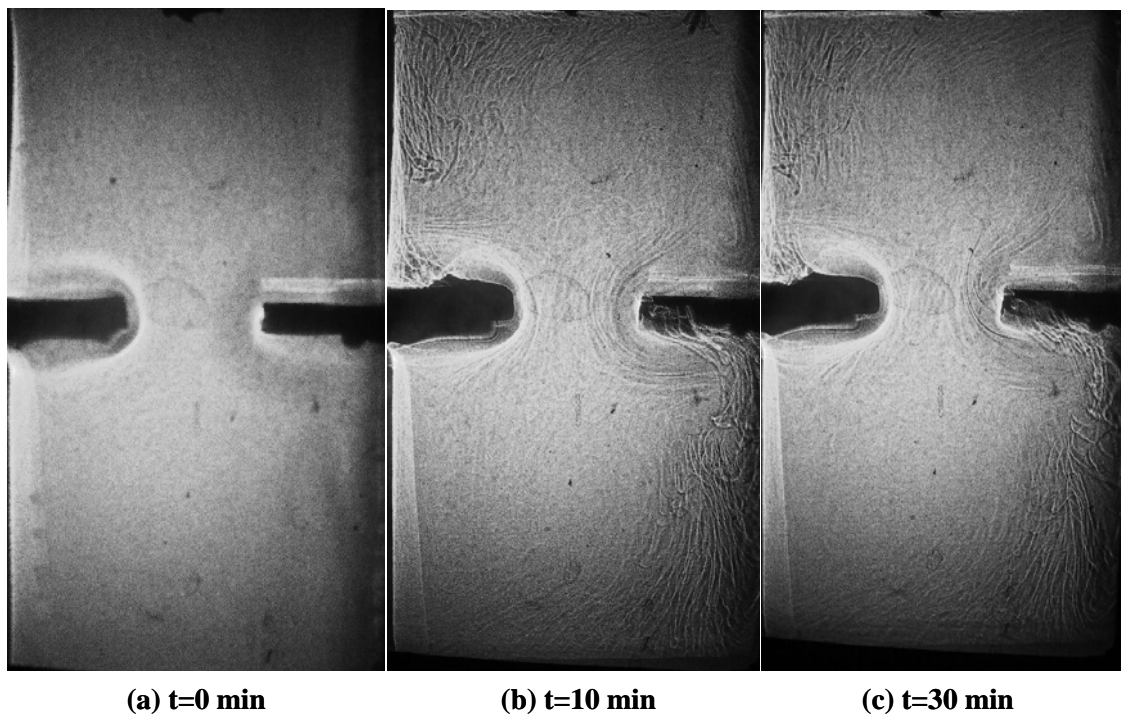
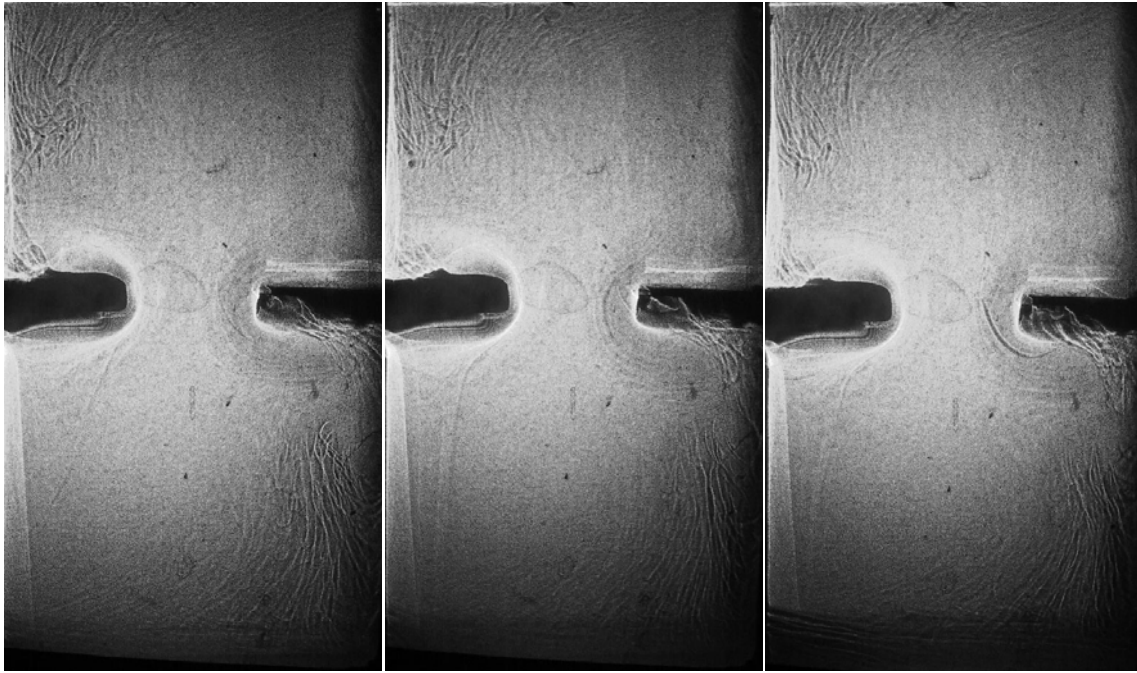


Fig.4. The boundary conditions of the rectangular enclosure

### Flow Structure

The effects of the flow pattern are determined by many factors, such as the thermal Grashof numbers, solutal Grashof numbers and the cell geometry. However, the step effects are emphasized herein. In the operating case with  $Gr_t=3.27 \times 10^6$  and  $N=10.68$  as shown in fig.5. the left plate is the cathode and the right plate is the anode . We can saw the enclosure, in the beginning, was dominated by thermal effect. The flow nearby the left-hot-plate moved to the top plate and then down to the right-cold-plate. In the meanwhile, the flow nearby the right-cold-plate moved downward to the bottom plate and then turn up to the left-hot-plate (fig. 5b). As the mass transfer time increases, the concentration effect dominated the enclosure. The hot and less dense fluid from left plate moved upward along the wall across the vertical middle-partition, and the cold and denser fluid moved downward along the wall across the vertical middle-partition. At  $t=60\text{min}$  (fig. 5d), the denser fluid began accumulates at the bottom plate (figs. 5a-f).





(d) t=60 min

(e) t=120 min

(f) t=180 min

**Fig.5. Flow pattern in cooperating case,  $Ar=2$ ,  $Ap=1/2$ ,  $Gr_t=3.27 \times 10^6$ ,  $Gr_m=3.49 \times 10^7$ ,  $N=10.68$**

In the opposing case with  $Gr_t=3.27 \times 10^6$  and  $N=-10.68$ , as shown in fig. 6, We can saw the enclosure, in the beginning, was dominated by thermal effect. The flow nearby the left-hot-plate moved to the top plate and then down to the right-cold-plate gradually became a cycle. As the mass transfer time increases, the thermal and solutal diffusion directions are in opposition, causing the two body forces to oppose one another. The finger type flow happened from both left and right plate. The physics of this formation are differ markedly from the physics in the cooperating case. Since the flow in the thermal boundary layer exerts a strong shear stress, the fluid from the hot anode in the solutal boundary is carried upward against the buoyancy force. This fluid acts downward in the solutal boundary. When this fluid reaches the top plate and leaves the thermal boundary layer, some denser fluid out of the thermal boundary moved downward and a finger-typed flow is observed (Fig. 6b). The accumulation happened near the left vertical middle-partition when the denser reaches. It was due to the length of the partitions and the trap effect. The same phenomenon is observed also near the right vertical middle-partition (figs. 6a-f).

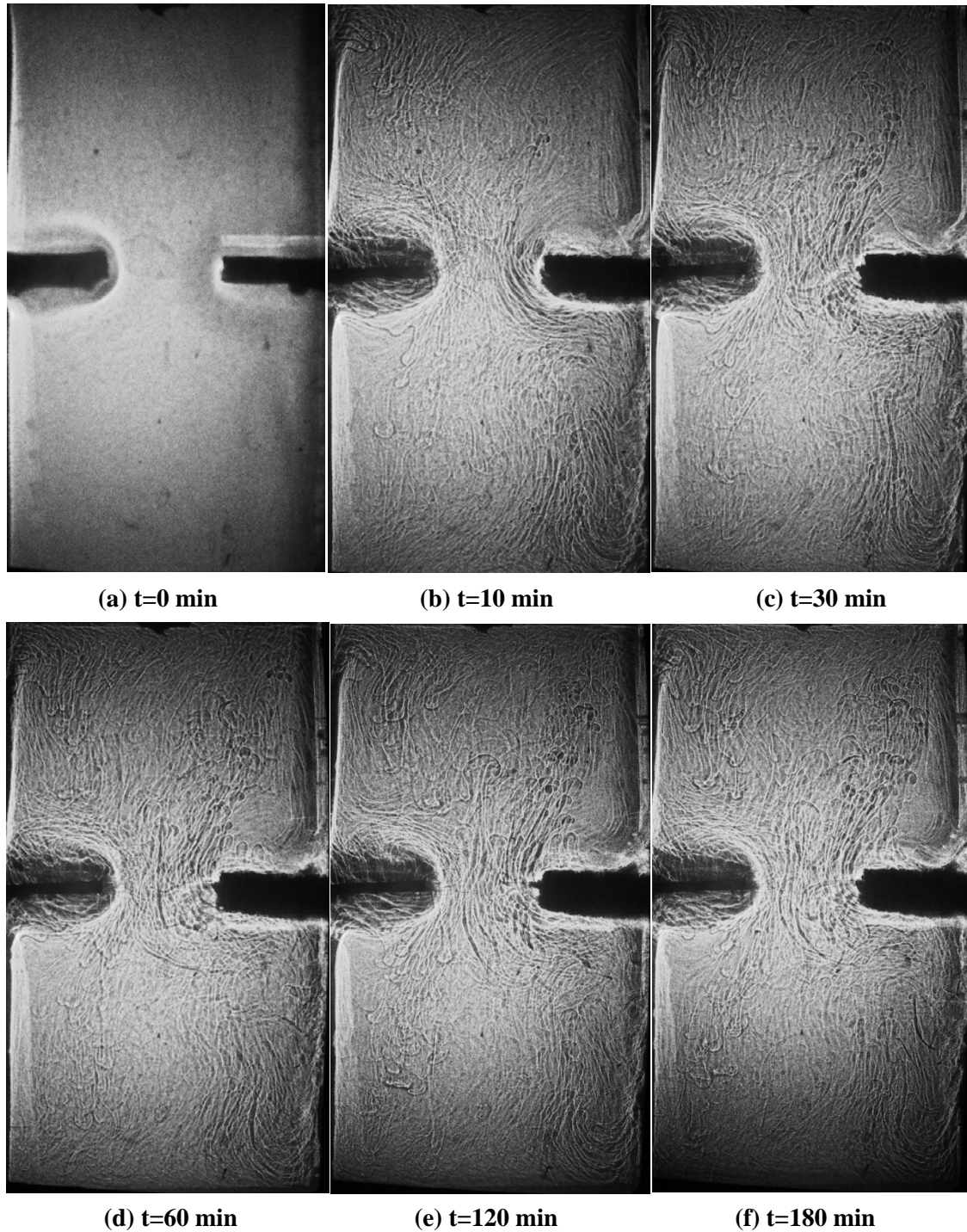


**Fig.6. Flow pattern in opposing case,  $Ar=2$ ,  $Ap=1/2$ ,  $Gr_t=3.27 \times 10^6$ ,  $Gr_m=3.49 \times 10^7$ ,  $N=-10.68$**

### **Mass Transfer Rate**

Thermosolutal convection mass transfer in the rectangular enclosure is examined. The mass transfer rate is determined at limiting current. The limiting current per unit area of the cathode ( $i_L$ ) can be measured and the mass transfer coefficient calculated using Eq. (7). The dimensionless mass transfer rate, called the Sherwood number, is defined as

$$Sh \equiv \frac{hc \times H}{D} \quad (8)$$

which corresponds to Nu in the heat transfer. For fixed  $Gr_m$  value and  $Ap$ ,  $Gr_t$  is varied to study the effect of thermal convection on the mass transfer. Fig. 7 displays the results in the two cases.

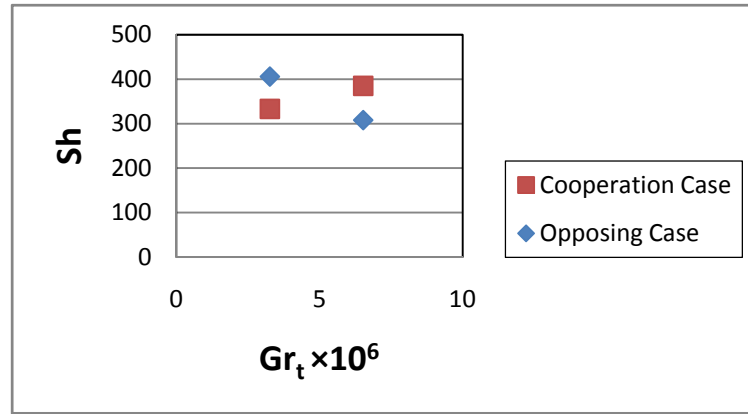


**Fig. 7. Correlation of  $Sh$  with  $Gr_t$  ( $Gr_m = 3.49 \times 10^7$ )**

In both cooperating and opposing cases,  $Sh$  increases with  $Gr_t$  for fixed  $Gr_m$  and  $Ap$  values, because increasing  $Gr_t$  strengthens the flows and thus monotonically increases  $Sh$ . Notably,  $Sh$  is larger in the cooperating case than in the opposing case for the same  $Gr_t \times 10^6$  and  $Gr_m$  values. The experimental error in the  $Sh$  value is estimated to be 10%.

## CONCLUSION

This experimental investigation examined how imposing concentration gradients affect steady thermal convection in a rectangular enclosure with vertical middle-partitions. The temperature and concentration gradients were imposed such that their effects on the flow cooperated or opposed. Double diffusive phenomena caused complex flow patterns to appear in a rectangular enclosure with vertical middle-partitions. In some cases, finger-type flows are observed in the layered flow structure.  $Sh$  (mass transfer rate) increased with  $Gr_t$  for fixed  $Gr_m$  and  $Ap$  values in the cooperating case.  $Sh$  was larger in the cooperating case than in the opposing case for the same  $Gr_t$  and  $Gr_m$  values.

## REFERENCES

- S. Ostrach (1980), "Natural Convection with Combined Driving Force," PCH:Physico Chemical Hydrodynamics, vol. 1, 233–247.
- L. W. Wang, Y. Kamotani and S. Ostrach (1983), "Experimental Study of Natural Convection in a Shallow Horizontal Cavity with Different End Temperatures and Concentrations," Rep. FTAS/TR-82-164, Case Western Reserve University, Cleveland, Ohio.
- Y. Kamotani, L. W. Wang, S. Ostrach and H. D. Jiang (1985), "Experimental Study of Natural Convection in Shallow Enclosures with Horizontal Temperature and Concentration Gradients," Int. J.

- Heat Mass Transfer, vol. 28, No. 1, 165–173.
- S. Ostrach (1982), “Fluid Mechanics in Crystal Growth-The 1982 Freeman Scholar Lecture,” J. Fluid Eng., vol. 105, 5–20.
- R. E. Powe, C.T. Carley and S.L. Carruth (1971), “A Numerical Solution for Natural Convection in Cylindrical Annuli,” J. Heat Transfer 92, 210–220.
- D. N. Mahony, R. Kumar and E.H. Bishop (1986), “Numerical Investigation of Variable Property Effects on Laminar Natural Convection of Gases between Two Horizontal Isothermal Concentric Cylinders,” ASME J. Heat Transfer, 108, 783–789.
- J. Dosch and H. Beer (1992), “Numerical Simulation and Holographic Visualization of Double Diffusive Convection a Horizontal Concentric Annulus,” Int. J. Heat Mass Transfer 35, 1811–1821.
- L. W. Wang and C. C. Chou (1991), “Experimental Study of Natural Convection Heat and Mass Transfer in an Annular Enclosure with a Cold Inner Cylinder,” Experimental Heat Transfer Vol.4, 367–380.
- L. W. Wang and C. Y. Wei (1992), “Thermosolutal Convection Heat and Mass transfer in a Vertical Annular Enclosure,” Experimental Heat Transfer Vol.5, 315–328.
- C. R. Wilke, M. Eisenberg, and C. W. Tobias (1953), “Correlation of Limiting Current under Free Convection Conditions,” J. Electrochem. Soc., vol. 100, 513–523.
- J. Newman (1991), Electrochemical systems, Prentice-Hall, Englewood Cliffs, New Jersey, USA.

## APPENDIX

### Notation

$b$	the charge number of the reacting ions.
$C_b$	bulk concentration of $\text{CuSO}_4$ (g-mole/cm <sup>3</sup> )
$\Delta C$	concentration difference between $C_b$ and $C_0$
$C_0$	ion concentration at the cathode
$D$	diffusion coefficient
$Gr_t$	thermal Grashof number ( $g\beta\Delta CH^3/\nu^2$ )
$Gr_m$	solutal Grashof number ( $g\bar{\beta}\Delta CH^3/\nu^2$ )
$F$	Faraday’s constant
$g$	gravitational acceleration
$h_c$	mass transfer coefficient
$i_L$	limiting current density (A/cm <sup>2</sup> )
$H$	high of the enclosure
$L$	depth of the enclosure
$W$	width of the enclosure
$S$	width of the partition
$d$	high of the partition

$Ap$	aperture ratio $(W-2S)/W$
$Ar$	aspect ratio $(H/W)$
$N$	buoyancy ratio $(\bar{\beta}\Delta C/\beta\Delta T)$
$Pr$	Prandtl number $(\nu/\alpha)$
$T$	temperature ( $^{\circ}\text{C}$ )
$T_c$	temperature of cold wall ( $^{\circ}\text{C}$ )
$\Delta T$	temperature difference between $T_h$ and $T_c$
$T_h$	temperature of hot wall ( $^{\circ}\text{C}$ )
$\alpha$	thermal diffusivity of the fluid ( $\text{cm}^2/\text{s}$ )
$\beta$	volumetric coefficient of thermal expansion $[-1/\rho(\partial\rho/\partial T)_c]$
$\bar{\beta}$	volumetric coefficient of solutal expansion $[1/\rho(\partial\rho/\partial T)_T]$
$\nu$	kinematic viscosity ( $\text{cm}^2/\text{s}$ )
$\rho$	fluid density ( $\text{g}/\text{cm}^3$ )